FEASIBILITY OF CO_2 INJECTION IN THE DEEP SALINE AQUIFERS OF THE BÉCANCOUR REGION, QUÉBEC (CANADA)

Tien Dung Tran Ngoc [(1)], René Lefebvre [(1)], Michel Malo [(1)] and Christine Doughty [(2)]

[(1)] Institut national de la recherche scientifique (INRS), Centre Eau Terre Environnement
490 rue de la Couronne, Québec, QC, G1K 9A9, CANADA
[(2)] Earth Sciences Division, E.O. Lawrence Berkeley National Laboratory
Berkeley, CA 94720, U.S.A.
E-mail: tien_dung.tran_ngoc@ete.inrs.ca

ABSTRACT

The feasibility of CO_2 injection in a reservoir of the Bécancour region was investigated using 2D radial numerical simulations with TOUGH2/ECO2N. To optimize the CO_2 injection rate and the duration of injection, we carried out sensitivity analyses considering different values of completion interval for the single injection well, rock compressibility, and the ratio of vertical and horizontal permeabilities. Simulations took into account Bécancour reservoir conditions, in which injection pressure was limited below the fracturing threshold, and sensitivity analyses provided indications of potential injection scenarios.

To remain below fracturing pressure, we propose intermittent 5-year injection periods, with a mass injection rate up to 20 kg/s, alternating with half-year periods without injection. This scenario may provide maximum CO_2 storage in the aquifer. We also calculated CO_2 storage capacities in different phases versus time. The effective apparent capacity and injection capacity estimated by the dynamic method, as well as effective storage capacity factors, were rigorously redefined on a mass and volume basis. For comparison purposes, CO_2 storage capacity was also estimated using volumetric and compressibility static methods. The storage efficiency factor obtained from the TOUGH2 dynamic method is about 1.5%, but it ranges between 2.2% and 3.3% for the static methods.

This study shows that the northeastern reservoir block of the Bécancour region could host ~10 Mt CO_2, which represents 15% to 50% of regional yearly CO_2 emissions over a few decades (depending on the injectivity scenario). Finally, this modeling study will also be the basis for the design of a pilot CO_2 injection test.

INTRODUCTION

According to a basin-scale assessment for different onshore and offshore basins in Southern Québec, Canada (Malo and Bédard, 2012)., the St. Lawrence Platform has the best potential for CO_2 storage in Quebec. Within the St. Lawrence basin**,** the Bécancour region, located between Montréal and Québec City along the St. Lawrence River, was selected for a site-scale study, because of data availability inherited from hydrocarbon exploration, as well as significant CO_2 production in the area (of about 1 Mt per year) from a cluster of stationary emitters. Deep saline aquifers in this region were characterized in terms of hydrogeology and petrophysics to assess their potential use for CO_2 sequestration. The brine-bearing sandstones of the Potsdam Group were recognized as the most favorable unit for a CO_2 injection (Tran Ngoc et al., 2011). The output of this characterization is summarized in this paper.

Based on a framework for the feasibility assessment of storage capacity, injectivity and integrity of specific sites, this paper presents the feasibility of supercritical CO_2 injection into the northeast reservoir block of the Bécancour region, using a series of 2D radial numerical simulations of multiphase flow and transport of H_2O-NaCl-CO_2 components. The parameterization analysis of hydrogeological properties controlling pressure buildup and CO_2 plume migration during and after injection (Doughty, 2010) is used with a dual purpose. On one hand, this sensitivity study offers an insight into the uncertainty related to our present knowledge of reservoir properties. On the other hand, the

relative advantages and disadvantages of conditions and properties at the Bécancour site as they relate to CO_2 storage are displayed by our simulation results and thus can now be compared to conditions and properties at other sites worldwide. Simulations provide estimated values for storage capacity, indicate potential storage injection scenarios (i.e., CO_2 distribution versus time) and feasible injection rates. This study also provides a comparison between CO_2 storage capacities estimated from several approaches.

SITE CHARACTERISTICS

The saline aquifers of the Bécancour region are part of the Paleozoic sedimentary succession of the St. Lawrence Platform, at depths ranging from 800 to 2400 m. Their lithostratigraphy, identified by well-log correlation and seismic line interpretation (Claprood et al., 2012), consists mainly of the following units: Potsdam Group (Covey Hill and Cairnside sandstones), Beekmantown Group (Theresa and Beauharnois dolostones) and Trenton Group (Chazy, Black-River and Trenton limestones). These saline aquifers are overlain by a cap rock of > 800 m thick shales and siltstones of the Utica Shale and Lorraine Group. The regional reservoir is separated by the SW-NE Yamaska normal fault into two faulted blocks found at different depths. In the present paper, we study CO_2 injection into the upper northeastern block of the fault.

All rock units are subhorizontal strata with excellent lateral continuity and small thickness variation. The units of the Potsdam Group, i.e., Covey Hill (CH) and Cairnside (CA) Formations, are the most porous, most permeable and thickest units of the sedimentary succession. Hydrogeological and petrophysical properties of these units are reported in Table 1. The fracturing pressure of Bécancour reservoir units was derived from minimal horizontal stress calculated in the St. Lawrence Platform basin (Konstantinovskaya et al., 2012). The compressibilities of Potsdam porous rock were determined from core measurements of porosity and net overburden pressures, and compared to literature values (Figure 1).

Capillary properties of Potsdam sandstones were based on measurements made on core samples using both mercury injection and capillary centrifuge tests. The van Genuchten (1980) model for capillary pressure (CP) and the Genuchten-Mualem (VGTM)/Corey model (Corey, 1954) for relative permeability (RP) was fitted to laboratory measurements (Table 2).

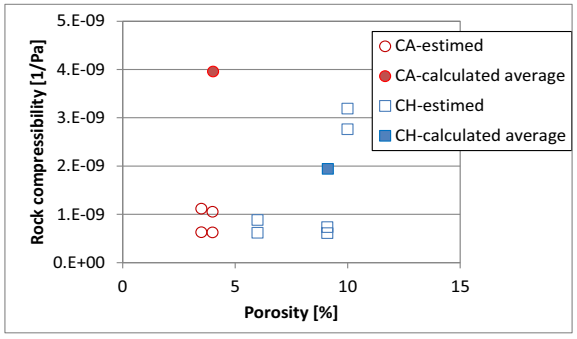

Figure 1. Correlation of rock compressibility with porosity for Covey Hill and Cairnside Fm. (values from empirical estimates and calculated from core measurements of porosity and net confining stress).

Table 1. Main representative properties of Covey Hill and Cairnside Fm.

Property	CH	CA
Porosity φ [%]	6.0	3.5
Horiz. permeability k_r [mD]	0.89	8.9
Vert. permeability k_z [mD]	0.12	0.06
Global permeability k [mD]	4.17/100[a]	
Pressure gradient ΔP_h [MPa/km]	12.17	
Min horiz. stress ΔS_{hmin} [MPa/km]	20.5	
Surface temperature $T_{surface}$ (°C)	8	
Temperature gradient ΔT [°C/km]	23.5	
Salinity *TDS* [g/l]	109	242
Rock compressibility c_r [1/Pa]	2×10^{-9}	4×10^{-9}

[a]: determined from drill stem tests for CA with 4.17 = geometric average and 100 = arithmetic average; 1 mD = 1×10^{-15} m^2.

Capillary properties for the CO_2-brine fluid system were obtained based on conversions from air-mercury and air-brine systems, using the experimental correlation of interfacial tension between CO_2 and brine proposed by Bachu and Bennion (2009). Figs 2 and 3 depict the capillary pressure and relative permeability

curves, respectively. Note that the residual liquid saturation S_{lr} [-] was estimated from sets of measured and deduced saturation values.

The residual gas saturation S_{gr} [-] was determined from Land's equation (Land, 1969), when assuming the liquid saturation at the drainage-to-imbibition turning point is equal to $S_{lcentral}$, the central saturation of the drainage branch, and S_{grmax} is the maximum saturation difference between the drainage and imbibition branches of capillary pressure curves.

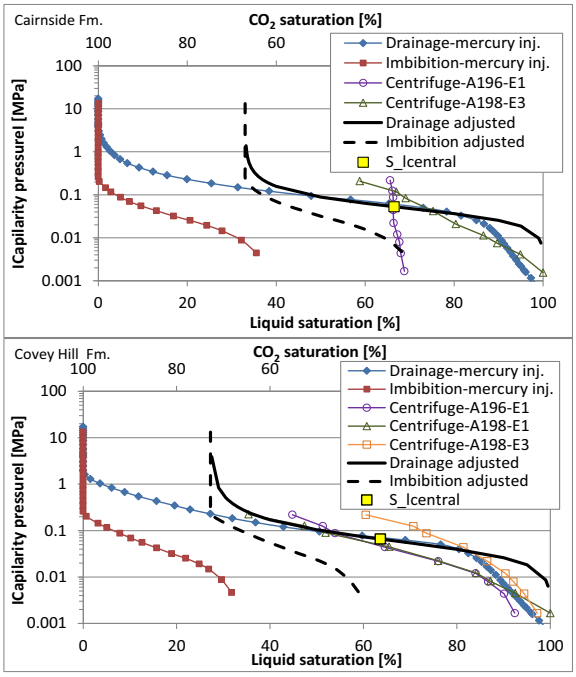

Figure 2. Capillary pressure as a function of fluid saturation for Covey Hill (lower) and Cairnside (upper) Fms.

Table 2. Capillary parameters of Covey Hill and Cairnside Fm. for the van Genuchten capillary model (drainage) and VGTM/Corey relative permeability model.

Capillary properties	CH	CA
Saturated liquid saturation S_{ls} [-]	1	1
Residual liquid saturation S_{lr} [-]	0.27	0.33
Residual gas saturation S_{gr} [-]	0.26	0.21
Exponent m [-]	0.558	0.621
Entry pressure P_{0cap} [Pa]	4.4×10^4	4.0×10^4

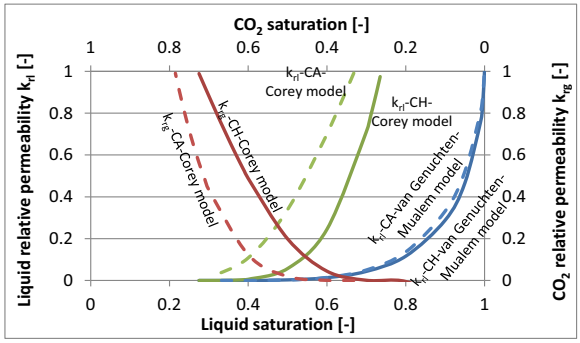

Figure 3. Relative permeability as a function of fluid saturation for CH (solid lines) and CA (dashed lines) Fm. according to the VGTM and Corey model.

NUMERICAL MODEL

The mathematical model of supercritical CO_2 injected and stored in deep saline aquifers was numerically implemented in TOUGH2/ECO2N (Pruess, 2005). We used this code for numerical simulations that were carried out in isothermal and non-hysteretic mode, considering transport only by convection from CO_2 injection and gravity. Certain processes were disabled, such as molecular diffusion, hydrodynamic dispersion, and permeability changes from salt precipitation, rock dissolution, or mineral carbonation.

Conceptual and numerical model

The area of the northeastern reservoir block targeted for CO_2 injection is referred as A [L^2], which is 7 by 5 km, equivalent to the circular surface with a radius of 3.3 km used in the model. The model consists of the Potsdam sandstones found at 1102–1503 m TVD with a thickness h [L] of 288 m for the Covey Hill Fm. and 113 m for the Cairnside Fm.

A two-dimensional (2-D) radial grid model was used to represent a cylindrical volume with central symmetry for the CO_2 storage site. Two homogeneous strata of Covey Hill and Cairnside sandstones are represented in the model, in which a vertical injection well is centered with an open-hole interval completed over the entire thickness of the Covey Hill Fm. A representative inner casing diameter of 0.15 m of other Bécancour boreholes was assumed for the injection well. Radial layers were discretized into 100 gridblocks, with finer meshing in the vicinity of the well using a logarithmic factor of ~1.085,

which allows us to create the radius of the first gridblock size equal to one of the injection wells. The vertical computational domain has a grid resolution of 25 layers (the Covey Hill Fm.) and 10 layers (the Cairnside Fm). All vertical cells are about 11 m thick.

Initial and boundary conditions

Table 3 summarizes the model initial conditions, based on site characterization data. All reservoirs above the Potsdam sandstones, together with cap rocks and the Grenville basement, are considered as sealing units. Therefore, the top and bottom of the model are impervious boundaries. Finally, CO_2 injection was presumed to be made into a closed volume system (Zhou et al., 2008).

Table 3. Initial and boundary conditions used for the Bécancour numerical model.

Initial conditions	CH	CA
Hydrostatic pressure P_{topCA} [MPa]	-	13.41
Temperature at top T_{top} [°C]	36.6	33.9
Salt mass fraction X [-]	0.098	0.195
CO_2 saturation [-]	0	0
CO_2 solubility in brine [g/l]	42.32	28.15
NaCl brine density [kg/m^3]	1140	1059
CO_2 density [kg/m^3]	801	803
NaCl brine viscosity [Pa.s]	1.2×10^{-3}	8.3×10^{-4}
CO_2 viscosity [Pa.s]	7.2×10^{-5}	7.3×10^{-5}
Boundary conditions		
Top z = - 1102 m:	no-flow	
Bottom z = - 1503 m:	no-flow	
Lateral r = 0:	mass injection	
Lateral r = 3300 m	no-flow	

Note: fluid properties correspond to the unit top

SENSITIVITY SIMULATION RESULTS

Simulations took into account Bécancour reservoir conditions in which injection pressure was limited below the fracturing pressure. This pressure is determined from thresholds for fracturing all rocks and displacing native caprock fluid by CO_2 (i.e. capillary pressure strength of caprocks) (Rutqvist et al., 2007). Here, the maximum sustainable injection pressure P_{max} stemmed from only S_{hmin} with a factor of 0.9 according to regulatory agencies, due to a lack of data on caprock units. The simulation base case used parameters from Table 1 and Table 2 with the Corey model for the relative permeability curves. Sensitivity analyses were carried out by varying only the Covey Hill parameters. Simulations considered injection periods of 5 to 50 years and a few hundred years thereafter, following stoppage of injection. We used the Petrasim interface for TOUGH2 simulations (Thunderhead-Engineering, 2010).

Hydrodynamic parameter effects

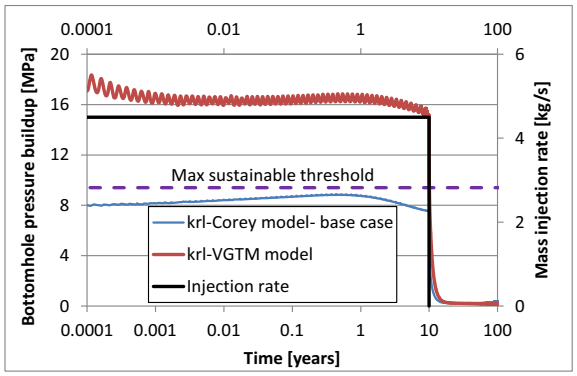

Figure 4. Pressure buildups versus time in the two cases using k_{rl} from the Corey model (base case) and VGTM model.

A mass injection rate of 4.5 kg/s for 10 years was applied at the injector for the base case without fracturing reservoir rocks. The pressure buildup would be double the maximum sustainable threshold ($0.9S_{hmin}$) if simulations used the k_{rl} of CH Fm. from the VGTM model (Figure 4). The overpressure of the base case (Corey k_{rl}) is smaller than the one for the case using VGTM k_{rl}, because the larger Corey k_{rl} (Figure 3) facilitates the displacement of injected brine by CO_2. The pressure transient for the case with VGTM k_{rl} has large oscillations, whereas it is very smooth for the case of Corey k_{rl}. This problem is not only attributed to discretization effects, but also to utilization of a hydrodynamic model. These oscillations occur due to density differences between phases whenever the CO_2 moves from one gridblock to the next in the radial direction. The oscillation effect may be attenuated with simulations using a 3D heterogeneous model.

The pressure buildup increases with a decrease of S_{gr} (not shown here), owing to the RP Corey model, in which k_{rl} decreases, i.e., overpressure increases, as S_{gr} decreases. The difference in the

overpressure is about 0.7 MPa between the two cases of $S_{gr} = 0$ and $S_{grmax} = 0.4$.

Petrophysical parameter effects

Injectivity is always proportional to reservoir permeability. Figure 5 shows the maximal injection rates with an injection period of 10 years as a logarithm function of the horizontal permeabilities k_r that are in the possible range for the target Covey Hill Fm. The maximal injection rate increases faster when $k_r < 5$ mD than $k_r > 5$ mD.

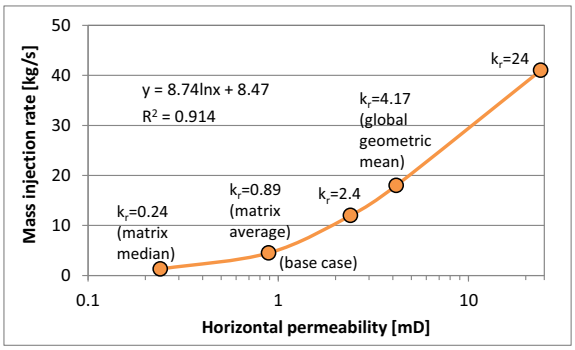

Figure 5. Injection rates used for 10 years as a function of horizontal permeability k_r of Covey Hill Fm.

For the vertical permeability k_z, well injectivity is not considerably changed due to bottomhole pressure buildup (not shown here) for k_z in the range from 0.012 to 1.2 mD. While k_z is not significant for the injection rate, its range of 0.01–0.1 mD being much less than k_r ($k_r/k_z = O(10^2)$) plays a role in delaying CO_2 buoyancy (not shown here). Thus, the storage formations themselves also contribute to secure sequestration of CO_2 by preventing upward migration.

Overpressures changed slightly in simulations (Figure 6) when estimated compressibility varied from 1×10^{-9} to 3×10^{-9} Pa^{-1}, comparable to the range of measured values (Figure 1). While the injection rate had only to be slightly decreased to 4 kg/s (from 4.5 kg/s for base case) to meet the sustainable threshold for the overpressure in the case using a Covey Hill compressibility of 2×10^{-10} Pa^{-1}, it could be increased to about 7 kg/s (factor of 1.5) for the case of 2×10^{-8} Pa^{-1}, and still not exceed the threshold (Figure 6).

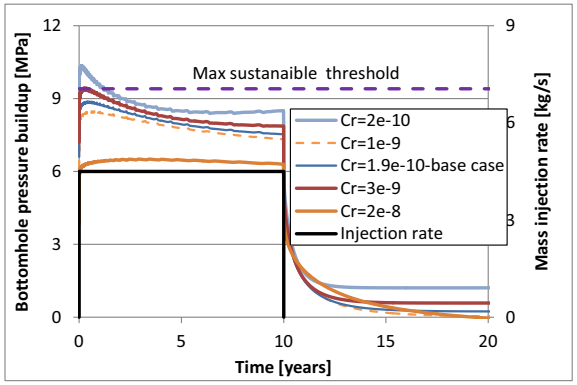

Figure 6. Pressure buildups versus time in the cases of Covey Hill Fm.'s different compressibility coefficients.

STORAGE SCENARIOS

Scenario description

The sensitivity analysis in the previous section shows that the base-case model parameters involve a certain robustness in the injection characteristics of the site. So, from the base case, scenarios of CO_2 injection are proposed that aim to assess reservoir storage capacity.

To use the maximum storage capacity of reservoirs, we tested the strategy of intermittent CO_2 injections. The injection rates and durations were estimated such that the induced aquifer pressures would not only be limited to the maximum sustainable pressure threshold of $0.9S_{hmin}$ within the injection periods, but also they would not exceed 1.3 P_h in the post-injection phase. Two proposed injection scenarios correspond to two cases of Covey Hill horizontal permeability, $k_r = 0.89$ mD and $k_r = 4.17$ mD. The latter belongs to the Cairnside Fm., but was used in simulations. While the small injection rates and a series of injection periods (~total 65 years) are applied in the case with $k_r = 0.89$ mD, the injection rates are large with only 3 injection periods in the case with $k_r = 4.17$ mD (~total 16.5 years) (Figure 7). The relaxation time between two intermittent injection periods is 0.5 years in both cases. It is not surprising that the cumulative injected CO_2 mass are at in the same order of magnitude regardless of the injection scenarios, considering the intrinsic storage capacity of the reservoir.

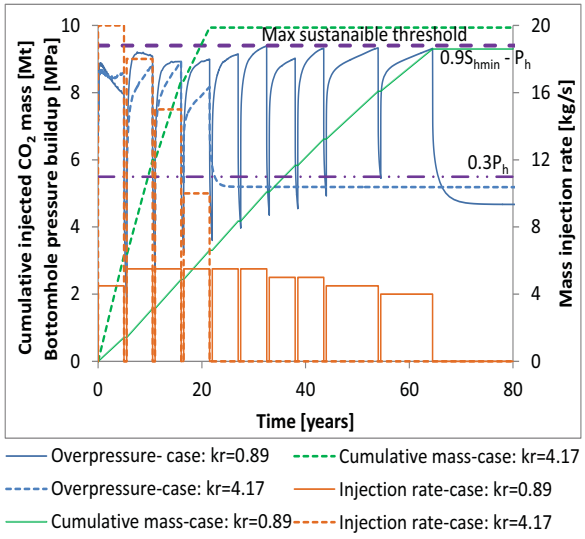

Figure 7. Overpressures at well bottom, injection rates and cumulative injected CO_2 mass versus time in two storage scenarios corresponding to the case with k_r = 0.89 and 4.17 mD respectively.

CO_2 plume migration

The spatial distribution of the supercritical CO_2 plume at t = 100 yrs for the two injection scenarios is presented in Figure 8. After the end of injection, the CO_2 plume migrates far from the injection point with only natural convection generated from the density difference between CO_2 and formation brine. In the scenario with k_r corresponding to the base case, the CO_2 front shows almost no advance in the Covey Hill Fm. beyond its extent at the end of injection, but there is continuous upward CO_2 migration in the Cairnside Fm. (Figure 9). CO_2 leaves the injection formation due to the permeability contrast between the two formations. This observation may be less visual in the scenario with CH k_r = 4.17 mD (Figure 8). Three hundred years after the onset of injection, injected supercritical CO_2 was detected at ~570 and 1130 m of radius of the cylindrically spreading plume in the Covey Hill and Cairnside Fm., respectively, for the case with CH k_r = 0.89 mD and ~680 and 950 m for the case with CH k_r = 4.17 mD.

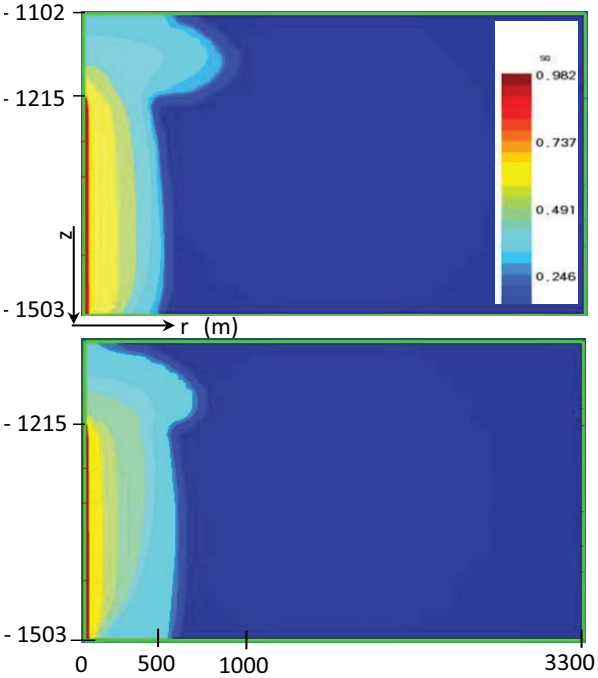

Figure 8. S_g CO_2 saturation at t = 100 years (after ~35 years of injection) in the injection scenarios with Covey Hill Fm. k_r = 0.89 mD (upper) and k_r = 4.17 mD (lower) (5 times vertical exaggeration).

ESTIMATIONS OF STORAGE CAPACITY

The CO_2 storage effective capacity for a potential site can be estimated by different methods using numerical simulations (dynamic methods) or analytic calculations (static methods). Consequently, the storage efficiency factor can vary considerably from one method to another. This section presents a number of estimates of storage capacity derived from various methods. For the purpose of comparison, the same input parameters were used for all methods as much as possible.

Definitions for dynamic method

The effective injection capacity M_{tot} [M] and apparent capacity V_{tot} [L^3] are defined on a mass and volume basis, respectively:

$$M_{tot} = M_{immisc} + M_{aq} = \langle S_g \rho_g \rangle \langle \phi \rangle V + + \langle S_l X_l^{CO_2} \rho_l \rangle \langle \phi \rangle V \quad (1)$$

$$V_{tot} = V_{immisc} + V_{aq} = \langle S_g \rangle \langle \phi \rangle V + n V_{partial} \quad (2)$$

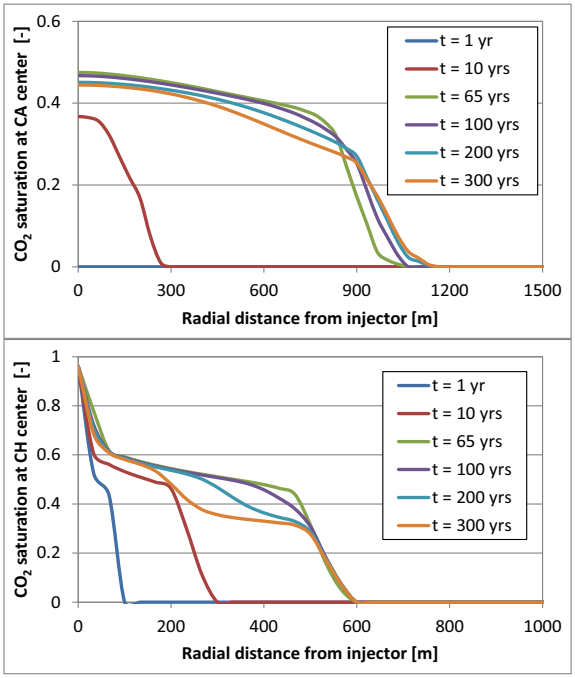

Figure 9. CO_2 saturation profiles at CA (upper) and CH (lower) central depth at different times in the injection scenario with k_r of the base case.

where M_{tot}/V_{tot} are the CO_2 total mass/volume that can be stored into the aquifers, M_{immisc}/V_{mmisc} are the mass/volume of immiscible CO_2 (gas-like phase) made up of the mobile CO_2 plume (M_{mob}/V_{mob}) and residual CO_2 trapped in pores (M_{immob}/V_{immob}) and M_{aq}/V_{aq} are the mass/volume of CO_2 dissolved in the aqueous phase. The sign < > stands for volume average over all domain (thus the "global" qualification used) taking into account the effect of formation geometry and heterogeneity. $V = A \times h$ [L^3] is the volume of aquifer (bulk volume). Note that V_{aq} is deduced from the apparent partial molar volume of CO_2 dissolved $V_{partial}$ [L^3 per mole], which only depends on the reservoir temperature (Pruess, 2005). n [mole] is the number of moles of CO_2 dissolved in the aqueous phase:

$$n = \frac{\langle S_l \, X_l^{CO_2} \rho_l \rangle \langle \phi \rangle V}{m_{CO_2}} \tag{3}$$

where m_{CO2} [M/mol] is the CO_2 molecular mass. TOUGH2/ECO2N simulations provides the variables used in Eqs. (1-2) and thus allow estimations of M_{tot}/V_{tot}, M_{immisc}/V_{mmisc}, and M_{aq}/V_{aq}.

From Doughty et al. (2001), the global storage efficient capacity factor C_{dyn} [-] is revisited as follows:

$$C_{dyn-\frac{mass}{vol}} = C_{g-\frac{mass}{vol}} + C_{l-\frac{mass}{vol}} \tag{4}$$

where $C_{g-\frac{mass}{vol}}$ (including C_{gmob} and C_{gimmob}) and $C_{l-\frac{mass}{vol}}$ [-] are efficiency factors of gas- and liquid-phase components. These factors can be defined on a mass or volume basis, assuming that the theoretical mass of CO_2 M_{theory} stored in the entire pore space saturated with a gas-like CO_2 phase corresponds to $C = 1$:

$$C_{g-mass} = \frac{M_{immisc}}{M_{theory}} = \langle S_g \rangle \tag{5}$$

$$C_{l-mass} = \frac{M_{aq}}{M_{theory}} = \langle S_l \, X_l^{CO_2} \frac{\rho_l}{\rho_g} \rangle \tag{6}$$

On a volume basis,

$$C_{g-vol} = \frac{V_{immisc}}{V_{pore}} = \langle S_g \rangle \tag{7}$$

$$C_{l-vol} = \frac{V_{aq}}{V_{pore}} = \frac{V_{partial}}{M_{CO_2}} \langle \rho_g \rangle \langle S_l \, X_l^{CO_2} \frac{\rho_l}{\rho_g} \rangle \tag{8}$$

where $V_{pore} = \langle \phi \rangle V$ [L^3] is the total pore volume of aquifer.

For the static methods, the US-DOE's (in Goodman et al, 2012) methodology is usually used to estimate the CO_2 storage capacity based on the volumetric or compressibility approaches. It is noteworthy that the volumetric approach only applies to an open-system, whereas the compressibility approach applies to a closed-system. In these methods, the pressure buildup is assumed spatially uniform (Zhou et al., 2008).

Results and comparison

From the TOUGH2 results obtained for the two injection scenarios (Figure 8), the evolutions with time of different forms of CO_2 are shown in Figure 10: dissolved CO_2 in liquid-phase, mobile and immobile CO_2 in gas-like phase of stored CO_2 mass. The storage capacity (290 kg per m^2) of the scenario with k_r = 4.17 mD is greater than that of the scenario with k_r base case (270 kg per

m^2) according to the contribution of all CO_2 forms in place within the injection time. Nonetheless, only the immobile CO_2 quantity (M_{immob}) is greater in the case with k_r = 4.17 mD than in the case with k_r of the base case after the end of injection, because the larger permeability allowed CO_2 to travel within a large zone in which much CO_2 was trapped as residual saturation. Dissolved CO_2 (M_{aq}) is almost the same in both scenarios and mobile CO_2 (M_{mob}) is slightly smaller in the case of k_r = 4.17 mD than in the case of k_r for the base case. Finally, the apparent capacity of the scenarios was expressed by ~1.1×10^7 m^3 of stored supercritical CO_2 or ~0.32 m^3 per m^2 of site surface (not shown).

Figure 11 presents the evolution of the storage efficiency factors versus time obtained on a mass and volume basis. As expected, the capacity factor of liquid phase is greater for the mass basis than in the volume basis, while the capacity factors of gas-phase remain the same for both approaches. Consequently, the global capacity factor is larger (but not by much) on a mass basis than for the volume basis. It can be seen that the increase in the capacity factors of dissolved and trapped CO_2, and the decrease in the capacity factor of free CO_2 with time, enhances the storage security of the site.

The storage capacity was also calculated by static methods after estimating efficiency factors (not shown here). The factors from the hydrodynamic contribution were estimated by using their relations to non-dimensional numbers such as the mobility ratio and capillary number proposed in the oil-gas engineering literature. The site storage capacity factor was obtained by using the mass basis. It is 3.3%, which falls within the range (0.51%–5.4% for clastic lithology) determined by the Monte Carlo probability (Goodman et al., 2011). Note that in the compressibility method, we estimated the efficiency factor (2.19%) when calculating the maximum pressure buildup at the center of formations, corresponding to $0.9S_{hmin}$.

The storage capacities of the northeastern reservoir block of the Bécancour region corresponding to the efficiency factors of all the estimates are shown in Figure 12. The stored CO_2 mass obtained from the TOUGH2 dynamic method is smaller than the one of the static methods. The difference is ~30% between the TOUGH and compressibility method and ~50%

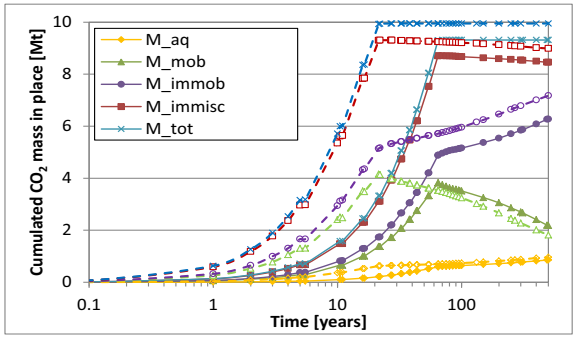

Figure 10. Evolution of different forms of cumulated CO_2 stored in place with time from the injection mass (solid lines for the injection scenario with k_r of the base case and dashed lines for k_r = 4.17).

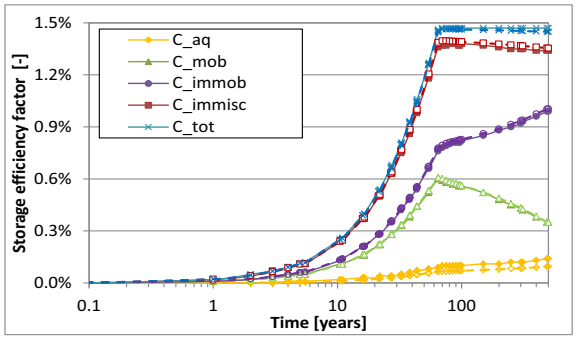

Figure 11. Capacity factors as a function of time for the scenario with k_r of the base case (solid lines for the mass basis and dashed lines for the volume basis).

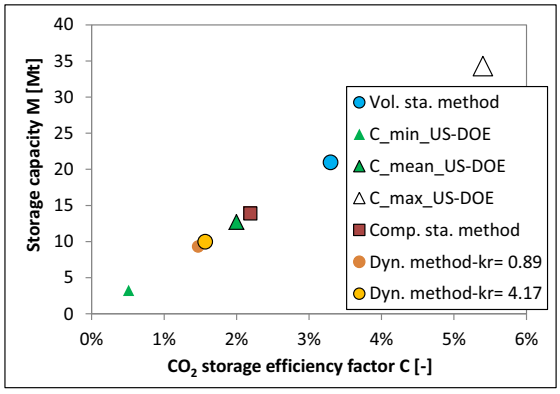

Figure 12. Storage capacity as a function of storage efficiency factors. Comparison between different estimation sources.

between the TOUGH and volumetric method. M_{tot} and $C_{dyn\text{-}mass}$ pairs of the dynamic method are linearly related between the storage capacity and efficiency factor. That reflects the fact that the theoretical mass of CO_2 stored in all the pore space M_{theory} is almost the same in all the methods, because the average CO_2 density over the entire reservoir domain by the TOUGH2 simulations is not much different from the estimated values in the static methods.

DISCUSSION AND CONCLUSIONS

The numerical sensitivity analysis documented in this paper highlights the influence of site properties, pressure constraints, and injection regime on the injection characteristics and thus the storage capacity. Permeability has the most direct impact on injectivity relative to other parameters (such as well diameter, thickness and depth of host formations, degree of CO_2 dissolution, compressibility, and permeability anisotropy), whereas capillary parameters have a global impact. In fact, simulation results for CO_2 injection could depend significantly on the capillary model used, at least for this study. The permeability contrast in the site favors preferential horizontal flow and impedes the upward migration of CO_2. From the point of view of security relative to CO_2 leakage risk, a compromise is needed between the completion interval and the injection rate in relation to vertical permeability. It is clear that greater rock compressibility plays a more important role for the aquifer pressure response. In this study, we did not investigate the sensitivity for the CA parameter, particularly for its permeability, for instance, CA k_r > CH k_r; this contrast could not force out the CO_2 plume remaining in the CH Fm. after the end of injections.

The injection strategy with intermittent and step-rates was applied in two proposed injection scenarios representing two cases: (1) $k_r < 1$ with long injection duration, and 2) $k_r > 1$ mD with short injection duration. The radial plume of injected CO_2 extended less than 1.2 km around the injection well. The total amount of CO_2 injection was on the order of 10 Mt for the two scenarios, which could be equivalent to regional emissions for ten years. Thus, the present geological sequestration option might consume 15%–50% of regional yearly CO_2 emissions in the few first decades from the start of injection. This annual emission of Bécancour would be all hosted in its deep saline aquifers by using vertical and/or horizontal multi-injectors.

The storage capacity estimated by the TOUGH2 simulations is smaller than the one obtained from static methods, because simulations take into account hydrodynamic multiphase processes that are not considered by static methods. It is also difficult to compare with the static volumetric method because of different hydraulic regimes. To compare with the static compressibility method, we modeled the aquifers as closed-system, which is suitable for Bécancour aquifers because no regional flow is observed and because it has small permeability. The efficiency capacity factors defined herein by the dynamic method are a function of time, but the global factor does not decrease after the end of injection. This is contrary to the efficiency capacity factor estimated for the reservoir with lateral spill points in Doughty et al. (2001). However, the local capacity factors, if calculated over a local domain (Doughty et al., 2002) in the closed aquifers, would increase or decrease with time. The application domain was defined for the storage capacity estimates and efficiency capacity factors of the TOUGH dynamic method.

The feasibility assessment of CO_2 injection in the deep saline aquifers of the Bécancour area (Québec) was carried out using TOUGH2 2D radial simulations, in which the injectivity and storage capacity estimates were investigated by the sensitivity study and the injection scenarios. A more detailed analysis will be presented in the forthcoming journal paper. These are the first numerical simulations showing the supercritical CO_2 behavior once the CO_2 is injected into the St Lawrence Lowlands salty sediment. This study is also a useful base for assessing seismicity induced by injection and leakage risk. A heterogeneous hydrodynamic model for the Bécancour reservoir will be developed on the basis of new data, especially the hydrogeology and petrophysical properties of cap rocks. The injection characteristics will be better mastered with the *in situ* permeability of the CH Fm. that will be established from field measurements. Finally, other processes involved in multiphase

flow and transport not yet taken into account in this study, such as capillary hysteresis, permeability modification, and diffusion-dispersion, are planned for future research.

ACKNOWLEDGMENT

We wish to acknowledge the Ministère du Développement durable, de l'Environnement et des Parcs du Québec (MDDEP) who financially supported this research.

REFERENCES

Bachu, S., and D. B. Bennion, Interfacial Tension between CO_2, Freshwater, and Brine in the Range of Pressure from (2 to 27) MPa, Temperature from (20 to 125) degrees C, and Water Salinity from (0 to 334 000) mg/L, *J Chem Eng Data*, *54*(3), 765-775, 2009.

Claprood, M., E. Gloaguen, B. Giroux, M. J. Duchesne, E. Konstantinovskaya, and M. Malo, Workflow using sparse vintage data for building a first geological and reservoir model for CO_2 storage in deep saline aquifer. A case study in the St. Lawrence Platform, Canada, *Greenhouse Gases: Science and Technology*, 2012.

Corey, A. T., The interrelation between gas and oil relative permeabilities, *Producers Monthly*, 38-41, 1954.

Doughty, C., Investigation of CO_2 plume behavior for a large-scale pilot test of geologic carbon storage in a saline formation, *Transport Porous Med*, *82*(1), 49-76, 2010.

Doughty, C., S. M. Benson, and K. Pruess, Capacity investigation of brine-bearing sands for geologic sequestration of CO_2, in *GHGT-6 Conference*, Kyoto, Japan, 2002.

Doughty, C., K. Pruess, S. M. Benson, S. D. Hovorka, P. R. Knox, and C. T. Green, Capacity investigation of brine-bearing sands of the Frio formation for geologic sequestration of CO_2, U.S. Department of Energy, National Energy Technology Laboratory, 2001.

Goodman, A., et al., US DOE methodology for the development of geologic storage potential for carbon dioxide at the national and regional scale, *Int J Greenh Gas Con*, *5*(4), 952-965, 2011.

Konstantinovskaya, E., M. Malo, and D. A. Castillo, Present-day stress analysis of the St. Lawrence Lowlands sedimentary basin (Canada) and implications for caprock integrity during CO_2 injection operations, *Tectonophysics*, *518*, 119-137, 2012.

Land, C. S., Calculation of imbibition relative permeability for two- and three-phase flow from rock properties, *SPE Journal*, *9*, 149-156, 1969.

Malo, M., and K. Bédard, Basin-scale assessment for CO_2 storage prospectivity in the Province of Québec, Canada, *Energy Procedia*, *in press*, 2012.

Pruess, K., *ECO2N: A TOUGH2 fluid property module for mixtures of water, NaCl, and CO_2*, LBNL-57952, 66 pp, Lawrence Berkeley National Laboratory, Berkeley, Calif., 2005.

Rutqvist, J., J. Birkholzer, F. Cappa, and C. F. Tsang, Estimating maximum sustainable injection pressure during geological sequestration of CO_2 using coupled fluid flow and geomechanical fault-slip analysis, *Energ Convers Manage*, *48*(6), 1798-1807, 2007.

Thunderhead-Engineering, *Petrasim user manual*, 124 pp, 2010.

Tran Ngoc, T. D., E. Konstantinovskaya, R. Lefebvre, M. Malo, and L. Massé, Geotechnical characterization of deep saline aquifers for CO_2 geological storage in the Bécancour region, Québec, Canada *Geotechnics for Sustainable Development-Geotec Ha Noi*, Construction Publishing House, Ha Noi, Viet Nam, pp. 623–632, 2011.

van Genuchten, M. T., A closed-form equation for predicting the hydraulic conductivity of unsaturated soils, *Soil Sci Soc Am J*, *44*(5), 892-898, 1980.

Zhou, Q. L., J. T. Birkholzer, C. F. Tsang, and J. Rutqvist, A method for quick assessment of CO2 storage capacity in closed and semi-closed saline formations, *Int J Greenh Gas Con*, *2*(4), 626-639, 2008.